

Quantum phase transitions in a two-dimensional quantum XYX model: Ground-state fidelity and entanglement

Bo Li, Sheng-Hao Li, and Huan-Qiang Zhou

Department of Physics and Centre for Modern Physics, Chongqing University, Chongqing 400044, People's Republic of China

(Received 22 December 2008; published 1 June 2009)

A systematic analysis is performed for quantum phase transitions in a two-dimensional anisotropic spin-1/2 antiferromagnetic XYX model in an external magnetic field. With the help of an innovative tensor network algorithm, we compute the fidelity per lattice site to demonstrate that the field-induced quantum phase transition is unambiguously characterized by a pinch point on the fidelity surface, marking a continuous phase transition. We also compute an entanglement estimator, defined as a ratio between the one-tangle and the sum of squared concurrences, to identify both the factorizing field and the critical point, resulting in a quantitative agreement with quantum Monte Carlo simulation. In addition, the local order parameter is “derived” from the tensor network representation of the system’s ground-state wave functions.

DOI: [10.1103/PhysRevE.79.060101](https://doi.org/10.1103/PhysRevE.79.060101)

PACS number(s): 05.70.Jk, 64.70.Tg, 03.67.—a

I. INTRODUCTION

Quantum critical phenomena are crucial in our understanding of the underlying physics in quantum many-body systems, especially in condensed-matter systems, due to their relevance to high- T_c superconductors, fractional quantum Hall liquids, and quantum magnets [1,2]. The latest advances in this area arise from quantum information science. Indeed, various entanglement measures have been widely applied to study condensed-matter systems. Remarkably, for one-dimensional (1D) quantum systems, von-Neumann entropy, as a bipartite entanglement measure, turns out to be a good criterion to judge whether or not a system is at criticality [3–9]. On the other hand, fidelity, another basic notion in quantum information science, has demonstrated to be fundamental in characterizing phase transitions in quantum many-body systems [10–13]. This adds a new routine to explore quantum criticality in condensed-matter physics from a quantum information perspective.

However, with only a few notable exceptions [14,15], not much work has been done for two-dimensional (2D) quantum systems due to great computational challenges. In fact, despite the existence of well-established numerical algorithms, such as exact diagonalization, quantum Monte Carlo (QMC), the density-matrix renormalization-group (DMRG) and series expansions, drawbacks become obvious when one deals with frustrated spin systems. A typical example is the QMC, which suffers from the notorious sign problem. However, a promising progress, inspired by new concepts from quantum information science, has been made in classical simulations of quantum many-body systems. The algorithms are based on an efficient representation of the system’s wave functions through a tensor network. In particular, matrix product states (MPSs) [16–18], a tensor network already present in DMRG, are used in the time-evolving block decimation (TEBD) algorithm to simulate time evolution in 1D quantum lattice systems [19,20], whereas projected entangled-pair states (PEPSs) constitute the basis to simulate 2D quantum lattice systems [21,22].

The aim of this Rapid Communication is to show that the fidelity per lattice site, introduced in Ref. [11], is able to

unveil quantum criticality for a 2D anisotropic spin-1/2 antiferromagnetic XYX model in an external magnetic field. This is achieved by exploiting tensor network algorithms, i.e., innovative algorithms inspired by the latest achievements in our understanding of quantum entanglement [21,22]. We show that the field-induced quantum phase transition is unambiguously characterized by a pinch point on the fidelity surface, marking a continuous phase transition. In addition, we compute an entanglement estimator, defined as a ratio between the one-tangle and the sum of squared concurrences (for all the pairwise entanglement between two spins), to identify both the factorizing field and the critical point, resulting in consistent conclusions as drawn from the fidelity approach, with an extra result about a factorizing field h_f . Our results are compared to those of the QMC simulation by Roscilde *et al.* [23] for the model. We stress that the QMC simulation is carried out for a system on a finite square lattice at very low but finite temperatures, whereas our simulation is directly performed for an infinite system at zero temperature.

II. QUANTUM XYX MODEL

We consider the 2D antiferromagnetic spin-1/2 XYX model in a uniform z -axis external magnetic field,

$$H = J \sum_{\langle i,j \rangle} (S_i^x S_j^x + \Delta_y S_i^y S_j^y + S_i^z S_j^z) + \sum_i h S_i^z, \quad (1)$$

where $J > 0$ is the exchange coupling, $\langle i,j \rangle$ runs over all the possible pairs of the nearest neighbors on a square lattice, and h is the external magnetic field. From the noncommutativity of the spin-1/2 Pauli operators, XYX model is expected to undergo a continuous quantum phase transition, with the same universality class as the 2D quantum Ising model in a transverse field. $\Delta_y < 1$ and $\Delta_y > 1$ correspond to easy-plane (EP) and easy-axis (EA) behaviors, respectively. The ordered phase in the EP (EA) case arises from spontaneous symmetry breaking along the x (y) direction, with a finite value of the order parameter, i.e., the magnetization m_x (m_y) below the critical field h_c . In Ref. [23], the QMC simulation was ex-

ploited to discuss the connection between quantum phase transitions and entanglement measures, where an entanglement estimator, defined as the ratio between the one-tangle and the sum of squared concurrences, was systematically analyzed to signal a quantum critical point.

III. INFINITE PROJECTED ENTANGLED-PAIR STATE METHOD

Let us briefly recall the infinite projected entangled-pair state (iPEPS) algorithm. Consider a finite two-dimensional square lattice where each site, labeled by a vector $\vec{r}=(x,y)$, is represented by a local Hilbert space $V^{\vec{r}}\cong C^d$ of finite dimension d . Let a vector $|\Psi\rangle$ denote a pure state in the (global) Hilbert space and the operator $H=\sum_{\vec{r},\vec{r}'}h^{\vec{r}\vec{r}'}$ be a Hamiltonian with the nearest-neighbor interactions on the lattice. Each lattice site has been represented by a tensor $A^{\vec{r}}$, so a PEPS for the state $|\Psi\rangle$ consists of a set of tensors $A^{\vec{r}}$. The tensor $A_{sudlr}^{\vec{r}}$ is made of complex numbers labeled by one *physical* index s and four *inner* indices $u, d, l, \text{ and } r$. The physical index runs over a basis of $V^{\vec{r}}$, so that $s=1, \dots, d$, whereas each inner index takes D values, where D is some bond dimension, and connects the tensor with the tensors in the nearest-neighbor sites. Thus, in a lattice with N sites, a PEPS depends on $O(ND^4d)$ parameters [21].

Now we move to a system defined on an infinite square lattice and assume that both $|\Psi\rangle$ and H are invariant under shifts by two lattice sites. We exploit this invariance to store the iPEPS using only two different tensors A and B . Given an iPEPS for a state $|\Psi_0\rangle$ (e.g., a product state), the iPEPS algorithm allows to perform an evolution in imaginary time to compute a ground-state wave function of a given Hamiltonian H , $|\Psi_\tau\rangle=e^{-H\tau}|\Psi_0\rangle/\|e^{-H\tau}|\Psi_0\rangle\|$ [22].

A contraction process, which is related to an evolution task, is done in order to get the effective environment for a pair of tensors A and B [22]. In practice, a global optimization problem has been reduced to a local two-site optimization problem. Two new tensors A' and B' could be computed by a sweep technique [17], originally devised for an MPS algorithm applied to 1D quantum systems with periodic boundary conditions [18].

IV. FIDELITY PER LATTICE SITE

Consider a finite 2D square lattice system described by Eq. (1), with the external magnetic field h as a control parameter. For two different ground states of the system, $|\Psi(h)\rangle$ and $|\Psi(h')\rangle$, corresponding to two different values h and h' of the control parameter, respectively, the fidelity per lattice site d is defined as

$$\ln d(h,h') = \frac{\ln F(h,h')}{N}, \quad (2)$$

where N is the system size and $F(h,h')\equiv|\langle\psi(h')|\psi(h)\rangle|$ is the ground-state fidelity. The fidelity per lattice site d depicts how fast the fidelity goes to zero when N gets large. Remarkably, the fidelity per lattice site d is well defined in the thermodynamic limit:

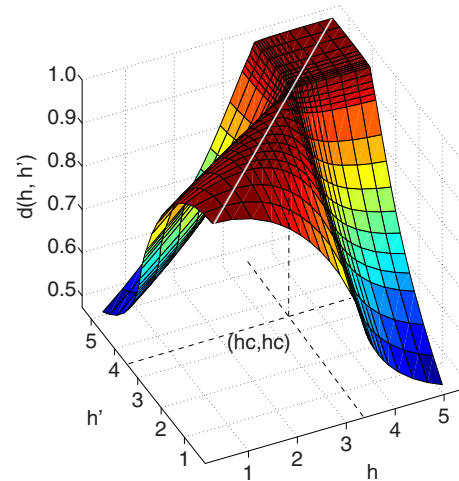


FIG. 1. (Color online) The fidelity per lattice site $d(h,h')$, as a function of h and h' for two ground states of the two-dimensional quantum XYX model. This defines a 2D fidelity surface embedded in a three-dimensional Euclidean space. A continuous phase transition point $h_c\approx 3.489$ is characterized as a pinch point (h_c,h_c) on the fidelity surface, as argued in Ref. [11]. Here we have taken the bond dimension $D=2$. The gray line denotes the normalization: $d(h,h)=1$.

$$\ln d(h,h') = \lim_{N\rightarrow\infty} \frac{\ln F(h,h')}{N}. \quad (3)$$

It satisfies the properties inherited from fidelity $F(h,h')$: (i) normalization $d(h,h)=1$, (ii) symmetry $d(h,h')=d(h',h)$, and (iii) range $0\leq d(h,h')\leq 1$.

As shown in Ref. [11], the fidelity per lattice site $d(h,h')$ succeeds in capturing nontrivial information about stable and unstable fixed points along renormalization-group flows. Specifically, the fidelity surface, defined by the fidelity per lattice site $d(h,h')$ as a 2D surface embedded in a three-dimensional Euclidean space, exhibits singularities when $h=h_c$ or $h'=h_c$. That is, $d(h,h')$ exhibits singular behaviors when h crosses h_c for a fixed h' or h' crosses h_c for a fixed h . Therefore, a phase transition point h_c is characterized as a *pinch point* [24] (h_c,h_c) for *continuous* QPTs, i.e., the intersection of two singular lines $h=h_c$ and $h'=h_c$.

The fidelity per lattice site may be computed from the iPEPS representation of the ground-state wave functions, following the transfer-matrix approach described in Ref. [14]. We plot $d(h,h')$ in Fig. 1, computed with the help of the iPEPS algorithm [22] with bond dimension $D=2$ (the result for $D=3$ is very similar to that for $D=2$). A pinch point on the fidelity surface defined by $d(h,h')$ as a function of h and h' clearly indicates a second-order phase transition. In addition, the two stable fixed points at $h=0$ and $h=\infty$ are characterized as the global minima of the fidelity surface (for a fixed Δ_s).

V. ONE TANGLE AND THE CONCURRENCE

We now exploit the iPEPS algorithm to extract the ground-state entanglement properties of the quantum XYX model on an infinite square lattice. We first compute the one-

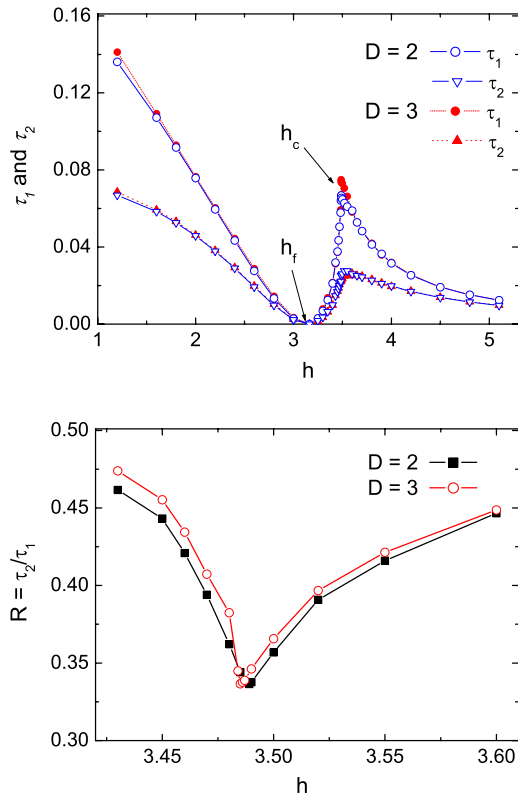


FIG. 2. (Color online) Upper panel: The one-tangle τ_1 and the sum of squared concurrences τ_2 as a function of an applied external field h for the 2D quantum XYX model with $\Delta_y=0.25$. The data are presented for both $D=2$ and $D=3$. The factorizing field, at which the one-tangle τ_1 vanishes, is indicated by an arrow labeled by h_f around 3.162. Above the factorizing field h_f , a steep increase in τ_1 and τ_2 reflects a rapid increase in entanglement around a critical point $h_c \approx 3.489$ ($D=2$) and $h_c \approx 3.485$ ($D=3$). Lower panel: an entanglement ratio $R = \tau_2/\tau_1$, exhibits a cusp, a signal of a continuous phase transition, at a critical point h_c obtained using the iPEPS algorithm with $D=2$ and 3. This is in an agreement with that resulted from the fidelity approach.

tangle τ_1 , defined as $\tau_1 = 4 \det \rho^{(1)}$, where $\rho^{(1)}$ is the single-site-reduced density matrix, for a specific value $\Delta_y=0.25$ with $D=2$ and 3. However, we stress that, our discussion, although only confined to the $\Delta_y=0.25$ case is actually quite generic and applies to all other values of $\Delta_y < 1$. The one tangle reflects the entanglement between a single site and the rest of the system. Note that there exists a factorizing field, at which the one-tangle τ_1 vanishes [25]. The exact theoretical value of the factorizing field $h_f = 2\sqrt{2(1+\Delta_y)}$ for $\Delta_y=0.25$ is approximately 3.162, consistent with the iPEPS results up to four digits. When the external field is increased beyond the factorizing field h_f , a cusp occurs for an entanglement ratio $R = \tau_2/\tau_1$ at a critical point h_c , where τ_2 denotes the sum of squared concurrences (for all the pairwise entanglement between two spins). The cusp in the entanglement ratio can be regarded as a signal of a quantum phase transition. In Fig. 2, both the one-tangle τ_1 and the sum of squared concurrences τ_2 , obtained from the iPEPS with $D=3$, are greater than those for $D=2$. This is due to the fact that for larger D , the PEPS representation accommodates more entanglement. The

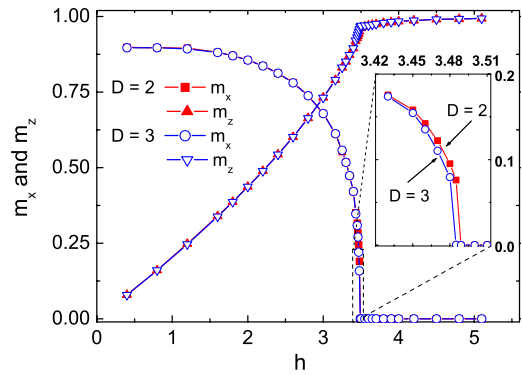


FIG. 3. (Color online) The x magnetization $m_x(h)$ in the ground state $|\Psi(h)\rangle$ of the 2D quantum XYX model ($\Delta_y=0.25$), a local order parameter, is readily read off from the iPEPS representation of the ground-state wave functions with $D=2$ and 3. Dashed lines are a guide to the eyes. For the external magnetic field h less than the critical magnetic field h_c , the order parameter takes a nonzero value and decays as h increases. Once the field is greater than the critical field h_c , the order parameter becomes zero. Notice that, around h_c , the derivative of the z magnetization $m_z(h)$ changes rapidly. Thus it exhibits singularities at the critical field h_c .

critical point $h_c \approx 3.485$ from the iPEPS for $D=3$ is smaller than that for $D=2$ ($h_c \approx 3.489$). The shift is quite small, so one may expect that the critical point for small D does not deviate significantly from the converged result with large D . Our result indicates that the iPEPS algorithm is able to capture the entanglement properties and gives rise to the results consistent with the QMC simulation.

VI. LOCAL ORDER PARAMETER

The efficient tensor network representation of the system's ground-state wave functions makes it possible to extract an (optimized) local order parameter, according to a general scheme advocated in Ref. [12]. In fact, once the critical field h_c is determined, one may choose two representative ground states, one for an external magnetic field h less than the critical field h_c and the other for an external magnetic field h greater than the critical field h_c . Then the reduced density matrix $\rho^{(1)}$ for a single lattice site in an infinite-size lattice is computed for two different values of the external magnetic field h , corresponding to $h > h_c$ and $h < h_c$, respectively. It is readily found that the one-site reduced density matrix $\rho^{(1)}$ displays different nonzero-entry structures in two phases, with $\langle S_x \rangle$ being zero for $h > h_c$ and nonzero for $h < h_c$. Also note that the Z_2 symmetry is spontaneously broken, since the reduced density matrix $\rho^{(1)}$ does not commute with the symmetry generating operator in the symmetry-broken phase $h < h_c$. This implies the existence of a local order parameter: $m_x = \langle \psi(h) | S_x | \psi(h) \rangle$, characterizing the second-order phase transition that belongs to the same universality class as that of the 2D quantum Ising model in a transverse field.

Another interesting local observable $m_z = \langle \psi(h) | S_z | \psi(h) \rangle$ is also carefully investigated, which exhibits singularities at the critical field h_c . If the external transverse magnetic field h is

raised from below the critical field h_c , then the z magnetization is a monotonic curve and gradually reaches a saturated value.

We plot m_x and m_z as a function of the external magnetic field h for the 2D quantum XYX model with $\Delta_y=0.25$ in Fig. 3. We have presented the data for both $D=2$ and 3, with the truncation dimension χ for iMPS used in the contraction of the iPEPS representation up to 30. On the other hand, although the factorizing field can be readily located in Fig. 2, there are no unusual features appearing in m_x and m_z around this point.

VII. CONCLUSIONS

We have performed a systematic analysis of both the ground-state fidelity and entanglement for the 2D quantum XYX model. This is achieved by computing the ground-state wave functions by means of the iPEPS algorithm. The results are compared with those obtained from the QMC simulation

[23], giving rise to a remarkable quantitative agreement for the factorizing field. From a fidelity perspective, a connection between a pinch point on the fidelity surface and a continuous phase transition point has been demonstrated, thus allowing us to determine the ground-state phase diagram of the 2D quantum XYX model. Once this has been done, one may read off the local order parameter from representative states in terms of the iPEPS representation of the ground-state wave functions.

An interesting point worth to be mentioned is that, in contrast to entanglement measures, the fidelity per lattice site fails to locate a factorizing field. However, one may resort to a closely related quantity, i.e., the so-called geometric entanglement introduced in Ref. [26], to locate it, as long as such a factorizing field exists for a system considered [27].

This work was supported in part by the National Natural Science Foundation of China (Grants No. 10774197 and No. 10874252).

-
- [1] S. Sachdev, *Quantum Phase Transitions* (Cambridge University Press, Cambridge, 1999).
- [2] X.-G. Wen, *Quantum Field Theory of Many-Body Systems* (Oxford University Press, Oxford, 2004).
- [3] J. Preskill, *J. Mod. Opt.* **47**, 127 (2000).
- [4] T. J. Osborne and M. A. Nielsen, *Phys. Rev. A* **66**, 032110 (2002); A. Osterloh *et al.*, *Nature* (London) **416**, 608 (2002).
- [5] G. Vidal, J. I. Latorre, E. Rico, and A. Kitaev, *Phys. Rev. Lett.* **90**, 227902 (2003); G. Vidal, *ibid.* **99**, 220405 (2007); G. Evenbly and G. Vidal, e-print arXiv:0710.0692.
- [6] V. E. Korepin, *Phys. Rev. Lett.* **92**, 096402 (2004); G. C. Levine, *ibid.* **93**, 266402 (2004); G. Refael and J. E. Moore, *ibid.* **93**, 260602 (2004); P. Calabrese and J. Cardy, *J. Stat. Mech.: Theory Exp.* (2004) P06002.
- [7] A. Kitaev and J. Preskill, *Phys. Rev. Lett.* **96**, 110404 (2006); M. Levin and X.-G. Wen, *ibid.* **96**, 110405 (2006).
- [8] F. Verstraete, M. A. Martin-Delgado, and J. I. Cirac, *Phys. Rev. Lett.* **92**, 087201 (2004); W. Dur *et al.*, *ibid.* **94**, 097203 (2005); H. Barnum *et al.*, *ibid.* **92**, 107902 (2004).
- [9] L. Amico *et al.*, *Rev. Mod. Phys.* **80**, 517 (2008).
- [10] P. Zanardi and N. Paunković, *Phys. Rev. E* **74**, 031123 (2006).
- [11] H.-Q. Zhou and J. P. Barjaktarevič, *J. Phys. A* **41**, 412001 (2008); H.-Q. Zhou, J.-H. Zhao, and B. Li, *ibid.* **41**, 492002 (2008); H.-Q. Zhou, e-print arXiv:0704.2945.
- [12] H.-Q. Zhou, e-print arXiv:0803.0585.
- [13] P. Zanardi, M. Cozzini, P. Giorda, e-print arXiv:cond-mat/0606130; N. Oelkers and J. Links, *Phys. Rev. B* **75**, 115119 (2007); M. Cozzini, R. Ionicioiu, and P. Zanardi, e-print arXiv:cond-mat/0611727 L. Campos Venuti, and P. Zanardi, *Phys. Rev. Lett.* **99**, 095701 (2007); P. Buonsante and A. Vezzani, *ibid.* **98**, 110601 (2007); W.-L. You, Y.-W. Li, and S.-J. Gu, *Phys. Rev. E* **76**, 022101 (2007); S.-J. Gu *et al.*, *Phys. Rev. B* **77**, 245109 (2008); M. F. Yang, *ibid.* **76**, 180403(R) (2007); Y.-C. Tzeng and M.-F. Yang, *Phys. Rev. A* **77**, 012311 (2008); S. Chen, L. Wang, Y. Hao, and Y. Wang, *ibid.* **77**, 032111 (2008); L. Campos Venuti, M. Cozzini, P. Buonsante, F. Massel, N. Bray-Ali, and P. Zanardi, *Phys. Rev. B* **78**, 115410 (2008); J. O. Fjærestad, *J. Stat. Mech.: Theory Exp.* (2008) P07011.
- [14] H.-Q. Zhou, R. Orús, and G. Vidal, *Phys. Rev. Lett.* **100**, 080601 (2008).
- [15] R. Orús, A. C. Doherty, and G. Vidal, *Phys. Rev. Lett.* **102**, 077203 (2009).
- [16] M. Fannes, B. Nachtergaele, and R. F. Werner, *Commun. Math. Phys.* **144**, 443 (1992); *J. Funct. Anal.* **120**, 511 (1994); S. Östlund and S. Rommer, *Phys. Rev. Lett.* **75**, 3537 (1995).
- [17] D. Perez-Garcia, F. Verstraete, M. M. Wolf, J. I. Cirac, *Quantum Inf. Comput.* **7**, 401 (2007).
- [18] F. Verstraete, D. Porras, and J. I. Cirac, *Phys. Rev. Lett.* **93**, 227205 (2004).
- [19] G. Vidal, *Phys. Rev. Lett.* **91**, 147902 (2003); **93**, 040502 (2004).
- [20] G. Vidal, *Phys. Rev. Lett.* **98**, 070201 (2007).
- [21] F. Verstraete and J. I. Cirac, e-print arXiv:cond-mat/0407066; V. Murg, F. Verstraete, and J. I. Cirac, *Phys. Rev. A* **75**, 033605 (2007).
- [22] J. Jordan, R. Orus, G. Vidal, F. Verstraete, and J. I. Cirac, *Phys. Rev. Lett.* **101**, 250602 (2008).
- [23] T. Roscilde, P. Verrucchi, A. Fubini, S. Haas, and V. Tognetti, *Phys. Rev. Lett.* **94**, 147208 (2005).
- [24] The terminology “pinch point” was introduced in Ref. [11].
- [25] This is due to the fact that there is no entanglement in a factorized state.
- [26] T.-C. Wei and P. M. Goldbart, *Phys. Rev. A* **68**, 042307 (2003); T. C. Wei, D. Das, S. Mukhopadhyay, S. Vishveshwara, and P. M. Goldbart, *ibid.* **71**, 060305(R) (2005).
- [27] The computation of the geometric entanglement per lattice site from a tensor network representation of the system’s ground-state wave functions is discussed in Q.-Q. Shi, R. Orús, J. O. Fjærestad, and H.-Q. Zhou, e-print arXiv:0901.2863; For matrix product states, see also, R. Orús, *Phys. Rev. Lett.* **100**, 130502 (2008).